Characteristics of Surface Micro-discharge Excited by Pulsed Voltage in Open Air

LI Dong, BAI Chuangfei, WANG Xiaohua, KONG Gangyu, LIU Dingxin
(State Key Laboratory of Electrical Insulation and Power Equipment, Xi'an Jiaotong University, Xi'an 710049, China)

Abstract: The surface micro-discharge (SMD) excited by pulsed voltage in open air is experimentally studied by measuring its voltage, current, emission image, emission spectrum, and ultraviolet (UV) absorption spectrum. It is found that the SMD occurs intermittently in each cycle, and that it consists of many filaments on the surface of grounded electrode. While the applied voltage's peak value U_p increases from 1.75 kV to 7.25 kV, the discharge area keeps expanding until $U_p \approx 6$ kV, when the discharge occupies all the available area. The emission spectrum of nitrogen metastable N_2(C-B) and the density of ozone increase almost linearly. The ozone density decreases hyperbolically downstream of the grounded electrode due to the diffusion in open air. The characteristics of pulsed SMD are presented and analyzed as well, which may be referred by further investigations.

Key words: surface micro-discharge; SMD; pulsed power; open air; ozone; emission spectrum
DOI: 10.3969/j. issn. 1003-6520. 2013. 09. 030 **Article No:** 1003-6520(2013)09-2273-07

0 Introduction

Cold atmospheric-pressure plasmas (CAPs) have received increasing attention due to theirs existing potential for various applications, such as environmental decontamination, surface functionization, and biomedicine[1-7]. Several kinds of discharge, such as dielectric barrier discharge, corona discharge, plasma jet, *etc.*, are often used for the generation of CAPs and massive efforts have been made in research and development of these discharges. However, surface micro-discharge (SMD) is less studied. This kind of discharge combines the nature of dielectric barrier discharge and corona discharge[8]. It can generate large-scale, macro-uniform, reactive CAPs in open air. It also has high safety because the plasma and the treated target are normally separated by a distance from mm to cm range. SMD provides an efficient, safe and cheap way as compared with other kinds of CAPs. It is much attractive for some applications, especially for plasma medicine.

In recent years, many investigations of SMD and its applications have been reported. Several different electrode configurations are developed, the electrical and optical characteristics are measured, and the plasma-induced species as well as their distributions are obtained[9]. The reactive oxygen species generated by SMD and used in biomedical applications, such as O_3 and reactive nitrogen species NO, are numerically and experimentally studied in both gas phase and the treated sample in downstream space (liquid phase)[10]. These reactive species are approved to play the key role in biomedical applications, and therefore enhancing their production efficiencies is of great interest. A possible way to achieve it is the use of pulsed voltage for the SMD excitation, instead of sinusoidal voltage. This approach has been approved to be valid for several kinds of CAPs, such as corona discharge[11], dielectric barrier discharge[12], plasma jet[13], *etc.* Moreover, the pulsed voltage may reduce the gas temperature in plasmas, which is also beneficial for the stability of SMD as well as its heat sensitive applications. However, so far there have been few reports of pulsed SMD, and hence little is known about its characteristics.

In this contribution, we report on an experimental study of pulsed SMD. The pulsed voltage and the discharge current of the plasmas are measured, and their characteristics are found to be closely related to the emission images taken by an intensified charge coupled device (ICCD). The emission spectroscopy and absorption spectroscopy are also used for measuring nitrogen metastable N_2(C-B) and O_3, respectively. The density and distribution of O_3 are obtained as a function of the excitation voltage. The characteristics of pulsed SMD are presented and analyzed in this study, which can be used as a reference for further investigations.

1 Experimental Setup

The experimental setup is shown in Fig.1. The SMD reactor consists of a plane active electrode, a mesh grounded electrode,

Project supported by Fundamental Research Fund for the Central Universities of China, State Key Laboratory of Electrical Insulation and Power Equipment (EIPE11108).

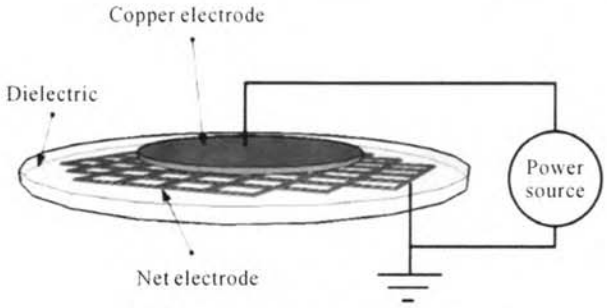

(a) SMD reactor and its corresponding circuit

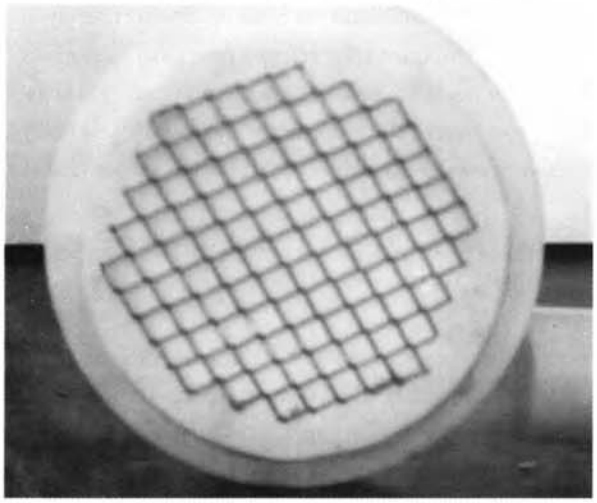

(b) Photo of the reactor

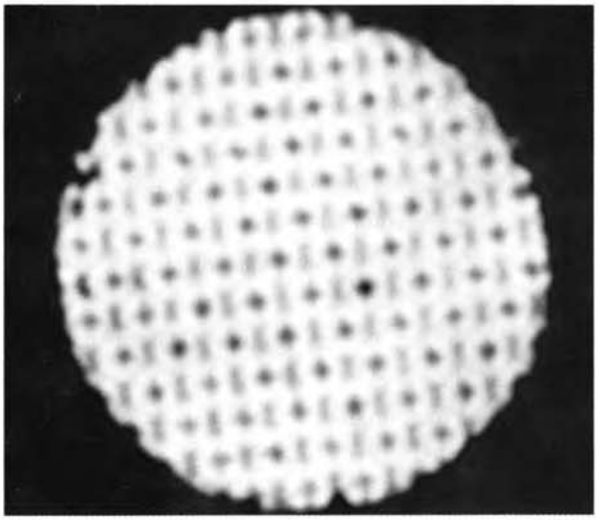

(c) Typical emission image of the plasma

Fig.1 Schematic diagram of the experimental setup

and a dielectric slab between the electrodes, as shown in Fig.1(a). A unipolar pulsed voltage is applied on the active electrode, with a pulse width of 13.5 μs and a frequency of 10 kHz (100 μs for each period). The power source (CTP-2000K/P) is produced by Moersi Electronics Co., Ltd. from Nanjing, China. A parallelogram mesh of stainless steel is used as the grounded electrode, as shown in Fig.1(b). The dielectric barrier is made by a polytetrafluoroethene (PTFE) board, with a thickness of 1.5 mm. The active electrode has a circular shape with diameter 8 cm, which is smaller than that of the grounded electrode. So, the image of discharge has similar shape as the one of the active electrode (see Fig.1(c)).

The voltage and current of SMD is measured by a high-voltage probe (Tektronix, P6015A) connected to the active electrode and a non-inductive resistance (30 Ω) in series with the grounded electrode. The waveforms are recorded by an oscilloscope (Tektronix, DPO3000). The temperature of the grounded electrode is measured by a thermocouple (Victor DM6801A). Two cameras are used to get the emission image of SMD, and their exposure times are much different. The first one is a common camera (Canon EOS7D) with an exposure time of milliseconds at least, and the other one is a ICCD (Andor, DH334T-18U-03) with a shortest exposure time of only 2 ns. The first one is used to get the macroscopic image of plasma, and since a single micro-discharge has a lifetime of a few ns[14], the ICCD is used to capture the filaments which occur alternatively.

The emission spectroscopy and absorption spectroscopy are performed for N_2(C-B) and O_3, respectively. The emission of N_2(C-B) is strong in air plasma, and, hence, its spectral lines 337 nm, 356 nm, 380 nm, *etc.*, can be used to indicate the intensity of SMD. Ozone is a strong oxidizer and a long-living molecule playing a key role in biomedical applications[15-16]. The density of O_3 is measured by using absorption spectroscopy at the wavelength of 253.7 nm[17]. In our work, a spectrometer (Ocean Optics, MAYA2000PRO) is used for the detection of spectral lines, and a deuterium lamp (DH2000, Ocean Optics) is used as a UV source for the absorption spectroscopy.

The deuterium lamp generates ultraviolet (UV) light with wavelength between 235 nm and 305 nm. The absorbance at 253.7 nm is measured to obtain the ozone density. The absorbance is given as[18]

$$\tau = -\ln\left(\frac{I - I_p - I_b}{I_0 - I_b}\right) \tag{1}$$

where, τ is the absorbance, I is the measured intensity with both the lamp and plasma on, I_p is when only the plasma on, I_0 is when only the lamp on, and I_b is when both the lamp and the plasma off (background noise). The line-of-sight averaged density of O_3 is obatined from the absorption spectrum according to the Beer-Lambert Law

$$\tau = \sigma \int_0^L n_{O_3}(r,z)\mathrm{d}r \tag{2}$$

where, $n_{O_3}(r,z)$ is the line-of-sight averaged density of ozone, cm^{-3}; σ is the photo absorption cross section $(1.14\pm0.01)\times10^{-17}$ cm^2[19]; L is the effective optical path of 8 cm.

The UV light is set to pass through the central axis downstream of the grounded electrode and parallel to the electrode surface at distances from 2 mm to 10 mm. The line-of-sight averaged density of O_3 is obtained as a function of downstream distance. The plasma is macroscopically homogeneous (exposure time about 1 s) (Fig.1(c)). So, it can be estimated that O_3 has a homogeneous density along the effective optical path, because it has a characteristic time larger than a discharge cycle by at least one order of magnitude.

2 Results and Discussion

2.1 Discharge evolution in one period

The waveforms of applied voltage and discharge current in one cycle are shown in Fig.2. The voltage has a peak value of about 5.6 kV, the full width at half maximum of the pulse is 13.5 μs, and the frequency is 10 kHz. There are many burrs in the current waveform, which indicates that the SMD is a typical micro-discharge. However, the burrs not always exist in the whole period (Fig.2(b)), which indicates that the micro-discharge occurs intermittently. Four regimes are defined according to the burrs, among which regimes 1 and 3 have no burr, and regimes 2 and 4 have burrs. Regime 1 has duration of 4 μs, and regime 2 has duration of 3 μs. These two regimes have the rising edge of voltage pulse. The current pulse in both regimes is about several ten of nanoseconds long. However, because the voltage is low in regime 1, it seems that the discharge is not ignited here (see Fig.2(a)). The discharge ceases as the applied voltage begins to decrease, which lasts for 6 μs (regime 3) until the voltage is below 2 kV. After that, the decrease of applied voltage slows down, and, therefore, the residual charge plays a role in igniting the micro-discharge again. The last phase (regime 4) has duration of 87 μs. However, the interval between two current pulses is much longer in regime 4 than that in regime 2.

In order to further explain the evolution of pulsed SMD, we plot in Fig.3 the emission images corresponding to the four regimes. The ICCD with an exposure time of 1 μs is used to capture the emission image. From several to several tens of images are obtained in these four regimes, and some of them are shown in Fig.3. As predicted by the discharge current (Fig.2(b)), it can be seen clearly that no discharge occurs in regime 1 and 3, and the filamentary discharges occur in turn in regime 2 and 4. Furthermore, no glow discharge occurs.

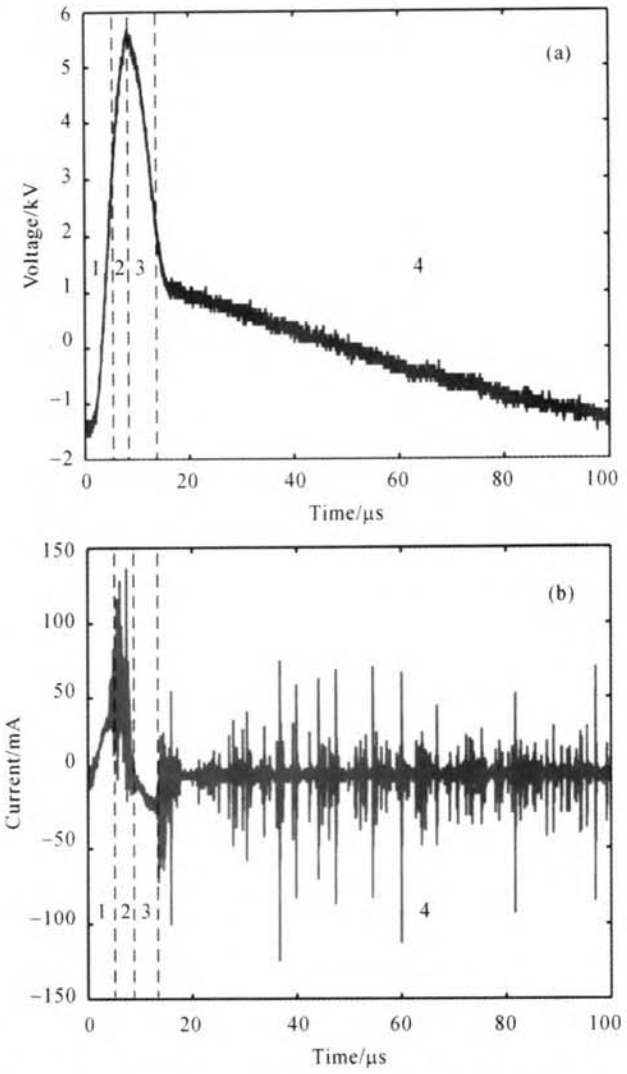

Fig.2 Waveforms of applied voltage and discharge current in one period of SMD

2.2 Effect of applied voltage on SMD

The emission images of SMD at different peak values of applied voltage, from U_p=2 kV to 7 kV with an interval of 1 kV, are shown in Fig.4. The images are obtained by Canon EOS7D camera with a long exposure time of 5 s. When the peak voltage is below 6 kV, it seems that the discharge area expands quickly with the increase of the applied voltage. The SMD occupies all the available area when U_p=6 kV. After that, the increase of applied voltage only results in increase of emission intensity. This phenomenon is similar to the radio frequency (RF) discharge, in which the discharge area expands at beginning, but, after occupation of electrodes, the plasma density increases with the applied voltage increase[20].

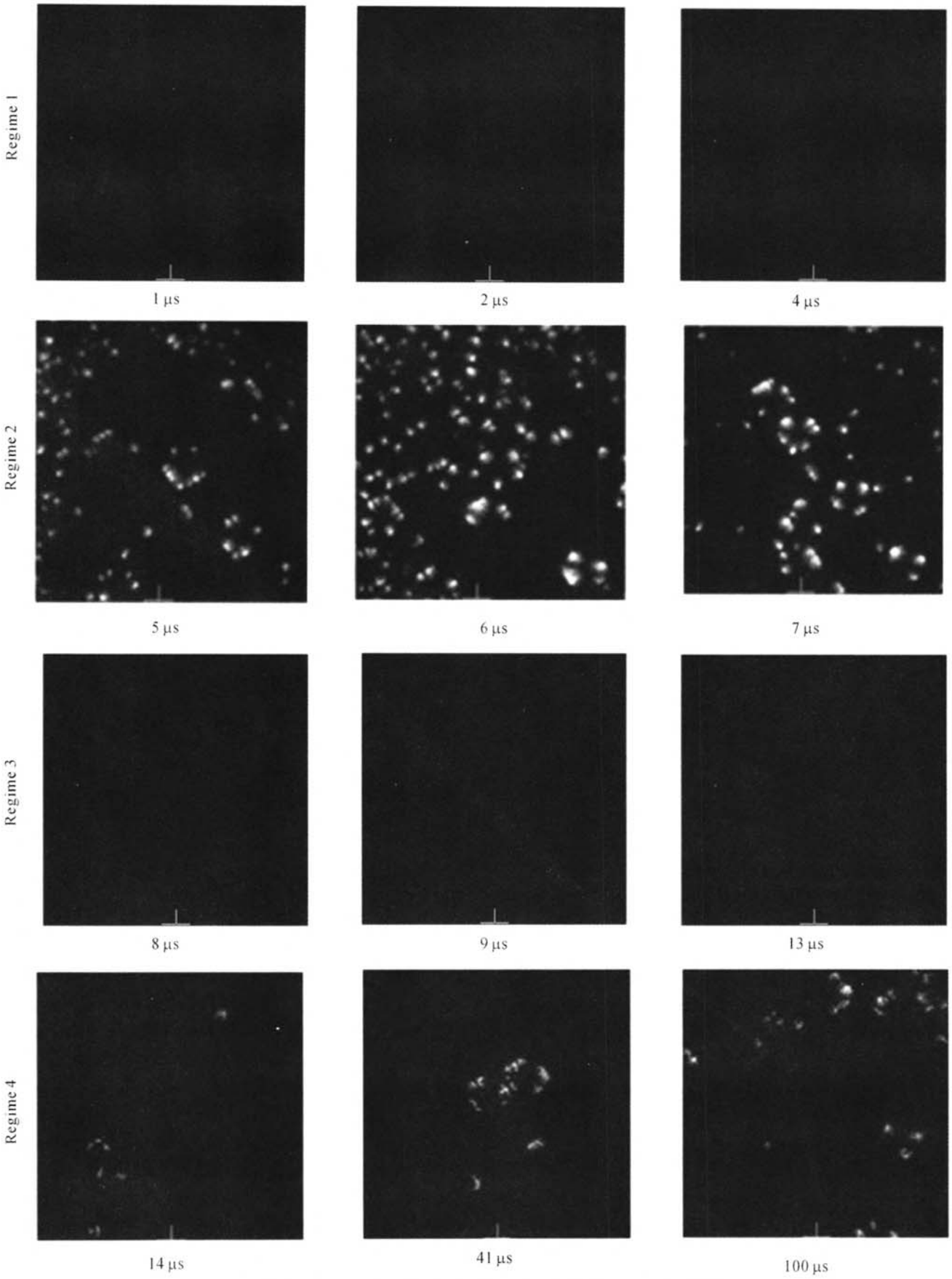

Fig.3 ICCD images of SMD regards to the four regimes of a period

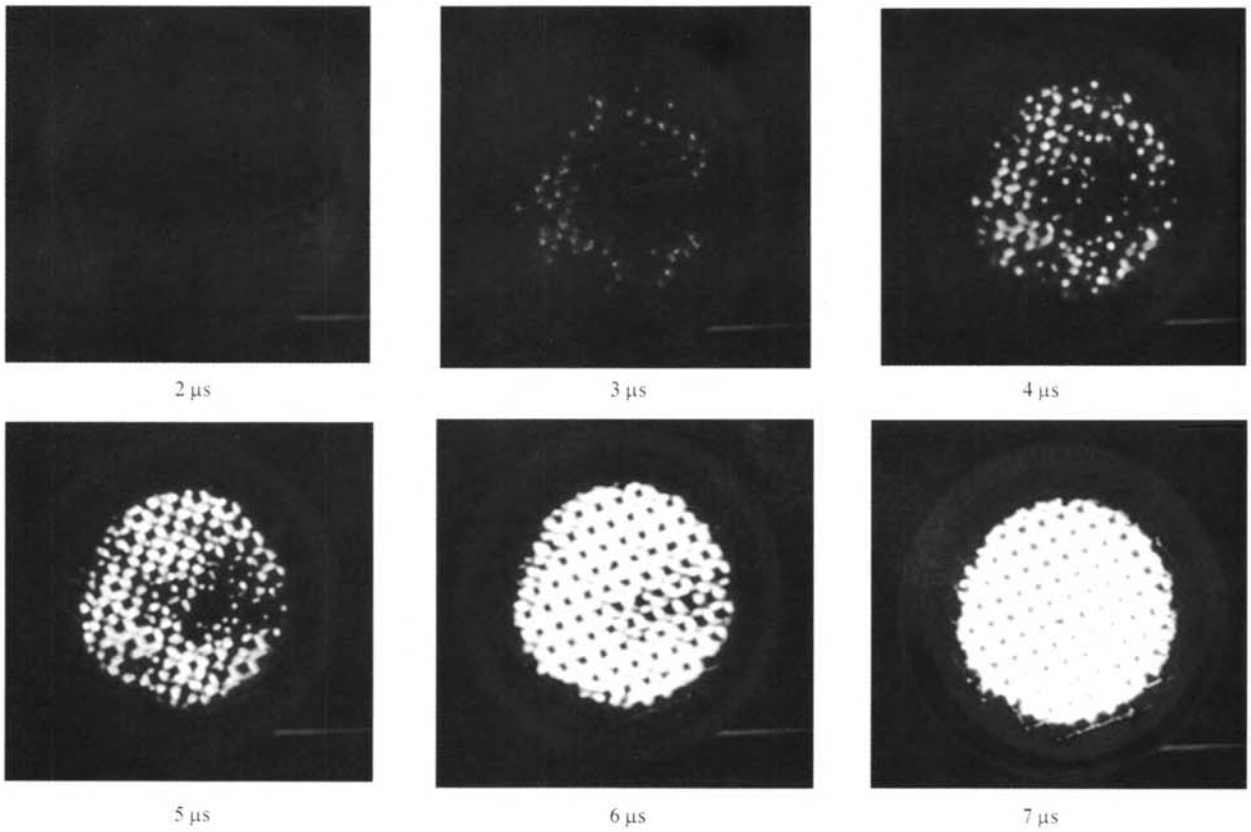

Fig.4 Images of SMD in several applied voltages

The input power and temperature of the grounded electrode are plotted in Fig.5 as a function of the applied voltage peak value varied from 1.75 kV to 7.25 kV. The input power and electrode temperature have similar behaviors, but the slope of input power curve is comparatively smaller when U_p<3.5 kV, and it turns to be bigger when U_p>5.5 kV. The slope of input power curve has three regimes: 1) the discharge is rarely happen when U_p<3.5 kV (see Fig.4) and hence the input power is nearly unchanged; 2) in the case of 3.5 kV<U_p<5.5 kV, the discharge area expands and hence restricts the dielectric slab temperature increase, which results in the fact that the dielectric property changes little and, in turn, limits the increase of input power; 3) the discharge occupies all the available area when U_p>5.5 kV, the temperature of dielectric slab increases sharply, and the dielectric property changes a lot in some area. Dielectric constant of PTFE decreases when the temperature increases. As a result, the input power increases sharply. In our experiments, the dielectric-slab (made by PTFE) exhibits breakdown when U_p>8 kV.

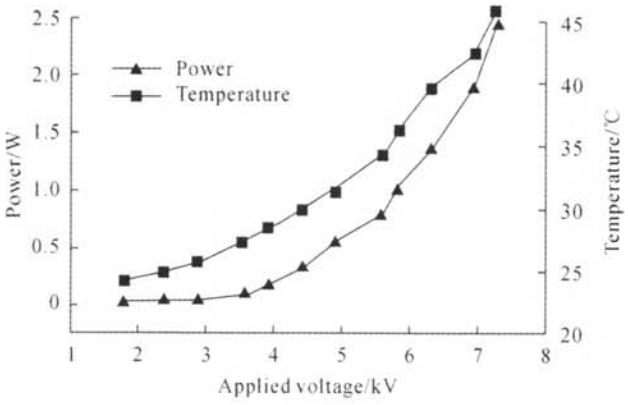

Fig.5 Input power and temperature rise of the ground electrode versus peak value of the applied voltage

2.3 Reactive species

The relative emission spectrum in the UV band is shown in Fig.6. Most of the spectral lines are observed in a wavelength range between 300 nm and 425 nm, which belongs to the transitions from second positive system of N_2[21]. The emission spectrum is similar to the other SMD studies, as reported by Morfill and Shimizu[8]. The relative intensity of spectral lines at 337 nm, 357 nm and 380 nm are plotted in Fig.7, with respect to the applied voltage peak values varied from 5.5 kV to 7.5 kV. It can be seen that the relative intensities of the spectral lines increase by 2.5 times, but the corresponding input power has even more increase of about 3 times. This indicates that the production efficiency of excited N_2 decreases with the rise of applied voltage, and that the additional increase of input power is consumed by the heating of gas and electrodes.

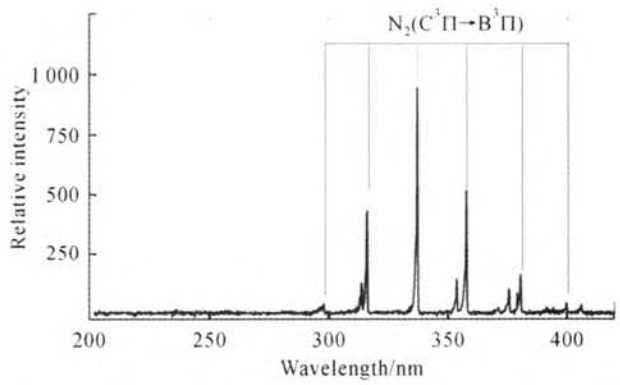

Fig.6 Emission spectrum of SMD in the wavelength range between 200 nm and 420 nm

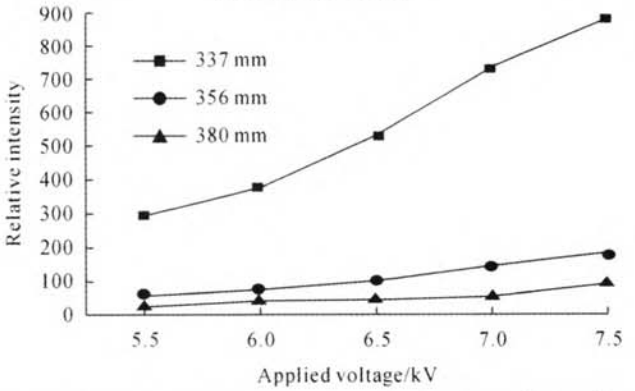

Fig.7 Relative intensities of different vibrational transitions of the N_2 2nd positive system as a function of applied voltage

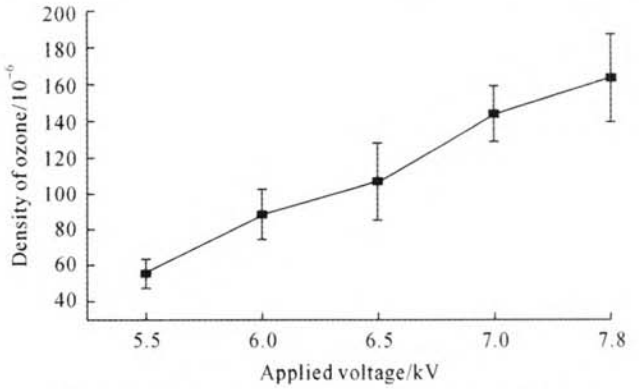

Fig.8 Density of ozone as a function of applied voltage

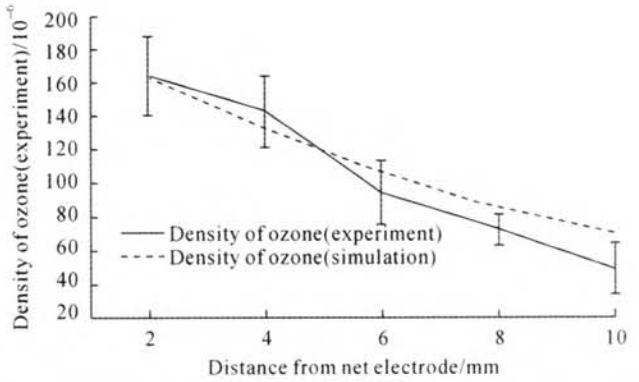

Fig.9 Density of ozone as a function of the distance from grounded electrode

Ozone is very important for various applications. Its density and distribution are measured in this study by using absorption spectroscopy. Fig.8 shows the line-to-sight averaged density of ozone at 2 mm downstream of the grounded electrode. The measurement is performed after 5 min of discharge in order to get the stable density, when the generation and loss of ozone due to diffusion and convection in open air is equal to each other. The density of ozone rises almost linearly with the peak value of applied voltage, from 55×10^{-6} to 164×10^{-6} (parts per million) with U_p variation from 5.5 kV to 7.5 kV. It was found that the density of ozone in SMD first increases and then decreases with the applied voltage[22]. However, in our study, the decrease does not occur until the discharge transits to spark. This may happen because: 1) pulsed voltage is used instead of sinusoidal voltage, and 2) the SMD is in the open air instead of a confined space.

In the downstream of the grounded electrode, the ozone density decreases hyperbolically downstream of the grounded electrode, as the distance from the electrode increases, as shown in Fig.9. Diffusion, convection and chemical reaction may have an effect on the density of ozone. We estimate that from 2 mm to 10 mm downstream of from the grounded electrode (see Fig.9) the diffusion dominates the loss of ozone. In order to prove our estimation, a simple 2-dimensional axisymmetric model is developed by considering only the diffusion process. The result is plotted as a dashed curve in Fig.9. It can be seen that the simulation and experiment have similar results, and hence the diffusion indeed dominates the loss of ozone in downstream area.

3 Conclusions

1) The surface micro-discharge (SMD) is a safe, cheap and efficient method as compared to other kinds of cold atmospheric-pressure plasmas. It is attractive especially for the burgeoning application in biomedicine. In this study, we use a pulsed voltage for the SMD generation, and the characteristics of the pulsed SMD are presented and analyzed.

2) The voltage, current, emission image, emission spectrum and UV absorption spectrum are measured. It is found that the SMD occurs intermittently in each cycle. It consists of many filaments that appear on the surface of grounded electrode. With the increase of applied voltage peak value U_p from 1.75 kV to 7.25 kV, the discharge area expands until $U_p\approx6$ kV, at which the discharge occupies all the available area. The emission spectrum of N_2(C-B) and the density of ozone increase almost linearly. The ozone density decreases hyperbolically

downstream of the grounded electrode as a result of the diffusion in open air.

Acknowledgment

The authors would like to thank Dr. NIE Qiuyue (Tsinghua University, China) for fruitful discussions related to this work.

References

[1] Laroussi M. Low temperature plasma-based sterilization: overview and state-of-the-art[J]. Plasma Processes and Polymers, 2005, 2(5): 391-400.

[2] Walsh J, Kong M G. Contrasting characteristics of linear-field and cross-field atmospheric plasma jets[J]. Applied Physics Letters, 2008, 93(11): 111501.

[3] Kong M G, Kroesen G, Morfill G, *et al*. Plasma medicine: an introductory review[J]. New Journal of Physics, 2009, 11(11): 115012.

[4] Fridman G, Beooks A, Balasubramanian M, *et al*. Comparison of direct and indirect effects of non-thermal atmospheric-pressure plasma on bacteria[J]. Plasma Processes and Polymers, 2009, 4(4): 370-375.

[5] FANG Zhi, CAI Lingling, LEI Xiao, *et al*. Surface treatment of polypropylene films using homogeneous DBD plasma at atmospheric pressure in air[J]. High Voltage Engineering, 2011, 37(11): 2746-2751.

[6] YANG An, NIE Qiuyue, WANG Zhibin, *et al*. Characteristics of the atmospheric pressure argon plasma jet[J]. High Voltage Engineering, 2012, 38(7): 1763-1769.

[7] LU Xinpei. Plasma jets and their biomedical application[J]. High Voltage Engineering, 2011, 37(6): 1416-1425.

[8] Morfill G, Shimizu T, Steffes B, *et al*. Nosocomial infections-a new approach towards preventive medicine using plasmas[J]. New Journal of Physics, 2009, 11(11): 115019.

[9] Pavlovich M, Chen Z, Sakiyam Y, *et al*. Effect of discharge parameters and surface characteristics on ambient-gas plasma disinfection[J]. Plasma Processes and Polymers, 2013, 10(1): 69-76.

[10] Matthew J P, Hung W, Sakiyam Y, *et al*. Ozone correlates with antibacterial effects from indirect air dielectric barrier discharge treatment of water[J]. Journal of Physics D: Applied Physics, 2013, 46(14): 145202.

[11] Xie G X, Yang Y, Luo J B, *et al*. AC pulse dielectric barrier corona discharge over oil surfaces: effect of oil temperature[J]. IEEE Transactions on Plasma Science, 2013, 41(3): 481-484.

[12] Williamson J, Trump D, Bletzinger P, *et al*. Comparison of high-voltage ac and pulsed operation of a surface dielectric barrier discharge[J]. Journal of Physics D: Applied Physics, 2006, 39(20): 4400-4406.

[13] Wu S, Huang Q, Wang Z, *et al*. On the magnetic field signal radiated by an atmospheric pressure room temperature plasma jet[J]. Journal of Applied Physics, 2013, 113(4): 043305.

[14] Kogelschatz U. Filamentary, patterned, and diffuse barrier discharge[J]. IEEE Transactions on Plasma Science, 2002, 30(4): 1400-1408.

[15] Khadre M A, Yousef A E, Kim J G. Microbiological aspects of ozone applications in food: a review[J]. Journal of Food Science, 2001, 66(9): 1242-1252.

[16] Eto H, Ono Y, Ogino A, *et al*. Low-temperature sterilization of wrapped materials using flexible sheet-type dielectric barrier discharge[J]. Applied Physics Letters, 2008, 93(22): 221502.

[17] Daumont D, Brion J, Charbonnier J, *et al*. Ozone UV spectroscopy, Ⅰ: absorption cross-sections at room temperature[J]. Journal of Atmospheric Chemistry, 1992, 15(2): 145-155.

[18] Winter J, Dunnbier M, Schmidt A, *et al*. Aspects of UV-absorption spectroscopy on ozone in effluents of plasma jets operated in air[J]. Journal of Physics D: Applied Physics, 2012, 45(38): 385201.

[19] Orphal J. A critical review of the absorption cross-sections of O_3 and NO_2 in the ultraviolet and visible[J]. Journal of Photochemistry and Photobiology A: Chemistry, 2003, 157(2): 185-209.

[20] Liu D, Iza F, Kong M G. Evolution of the light emission profile in radio-frequency atmospheric pressure glow discharges[J]. IEEE Transactions on Plasma Science, 2008, 36(4): 952-953.

[21] Shimizu K, Ishii T, Blajan M. Emission spectroscopy of pulsed power microplasma for atmospheric pollution control[J]. IEEE Transactions on Industry Applications, 2010, 46(3): 1125-1131.

[22] Shimizu T, Sakiyama Y, Graves D, *et al*. The dynamics of ozone generation and mode transition in air surface micro-discharge plasma at atmospheric pressure[J]. New Journal of Physics, 2012, 14(10): 103028.

LI Dong was born in Zhejiang province, China, in 1989. He received the B.S. degree in electrical engineering from Xi'an Jiaotong University, Xi'an, China, in 2012. He is currently working toward the PH.D degree in Xi'an Jiaotong University, Xi'an.

BAI Chuangfei received the B.S. degrees in electrical engineering from Xi'an Jiaotong University, Xi'an, China, in 2007 and 2011, respectively. He is currently working toward the M.S. degree in the School of Electrical Engineering, Xi'an Jiaotong University, Xi'an.

WANG Xiaohua received the B.Sc. from Chang'an University in 2000, and Ph.D. degree from Department of Electrical Engineering of Xi'an Jiaotong University in 2006. He is currently the professor with the same University. His research fields have been involved in low-temperature plasmas and their applications, On-line monitoring of electrical apparatus.

KONG Gangyu received the B.Sc. and M. Sc. from Zhejiang University in 1984 and 1987, respectively. He received the Ph.D. degree from Liverpool University in 1992. He is currently the professor with the centre for plasma medicine in Xi'an Jiaotong University.

LIU Dingxin (Corresponding author) received the B.S. and Ph.D. degrees from Xi'an Jiaotong University in 2004 and 2010, respectively. He is currently the lecturer with the same university. His research fields have been involved in low-temperature plasmas and their biomedical applications.
E-mail: liudingxin@gmail.com

Received date 2013-05-26
Editor LI Dong

作者： ， LI Dong， BAI Chuangfei， WANG Xiaohua， KONG Gangyu， LIU Dingxin
作者单位： State Key Laboratory of Electrical Insulation and Power Equipment, Xi'an Jiaotong University, Xi'an 710049, China

刊名： 高电压技术 ISTIC EI PKU
英文刊名： High Voltage Engineering
年，卷(期)： 2013,39(9)